

Softening Mechanism of Coherent Phonons in Antimony Under High Density Photoexcitation

H. Kumagai, I. Matsubara, J. Nakahara, and T. Mishina*

*Department of Physics, Faculty of Science,
Hokkaido University, Sapporo 060-0810, Japan*

(Dated: March 4, 2024)

Abstract

We have investigated the dynamical properties of coherent phonons generated in antimony under high density photo excitation. Precise measurements and extended analysis of coherent phonon oscillations provide new insights into the process of impulsive softening. In the process of recovering from instantaneous softening, phonon frequency shows an unexpected temporal evolution involving an abrupt change and a slight overshoot. Moreover, fluence dependence of the initial phonon frequency is strongly correlated with the phonon frequency shift of the high-pressure Raman spectra. These results clearly prove that the structural changes (lattice contraction and expansion) induced by laser excitation governs the softening mechanism of coherent phonons.

Photoexcitation of materials with intense femtosecond laser pulses has led to a unique physical process in various materials on a femtosecond time scale. For example, phase transition [1], laser ablation [2–4], laser melting [5, 6], and band-gap renormalization [7, 8] have been intensively studied. Softening of coherent phonons under high density excitation is one of the most important and promising phenomena to investigate. In addition to the continuous efforts to clarify the generation and detection mechanism of coherent phonons of various materials [9–11], their softening mechanism under high density excitation has been intensively focused. Early observations of the softening of coherent phonons in antimony and tellurium have been reported, and the mechanisms have been deduced as ionic screening by photoexcited carriers and purely electronic softening of the crystal lattice, respectively [12, 13]. Hase *et al.* have proposed that the softening mechanism involves anharmonicity of the lattice potential instead of electronic softening of the crystal lattice [14]. The effect of photoexcited electron-hole plasma on the phonon dispersion relation of bismuth has been investigated using first principles density-functional perturbation theory, and its influence on phonon softening also has been discussed [15]. Recently, time-resolved X-ray diffraction experiments have revealed the atomic motion of bismuth under phonon softening conditions [16]. However, the existing experimental evidence is still insufficient to arrive at a final conclusion on the phonon softening mechanism.

In this study, we explore the precise measurement of coherent phonon oscillations in antimony under high density excitation and examine the details of time evolution of frequency shifts. Time evolution exhibits an abrupt change and a slight overshoot, which are hardly expected from a carrier-phonon interaction. Moreover, fluence dependence of the initial frequency is closely correlated with the high-pressure Raman experimental results. The correlation is well explained by the theory based on the quantum motion of nuclei under intense excitation of bonding electrons. These results clearly prove that the structural changes induced by laser excitation govern the softening mechanism of coherent phonons.

The sample used in our experiment is a single crystal of antimony, with its surface perpendicular to the trigonal axis. Our experiments are performed in a reflection-type pump-probe system at room temperature. A commercial Ti:sapphire oscillator operating at repetition rates of 80 MHz and pulse width of 100 fs is used as the excitation light source. The pump and probe beams are orthogonally polarized to each other and they are coaxially arranged using a polarization beam splitter. The beams are focused on the sample to a diameter of

about $3\mu\text{m}$ with a microscope objective lens having a focal length of 4.5 mm. A high density excitation condition of maximum $20\text{ mJ}/\text{cm}^2$ is easily achieved in this configuration. In one series of measurements, the pump pulse width is controlled with a prism pair compensator so that the amplitude of the coherent phonon is varied without changing the fluence. The signal is averaged by a rapid scan system with an optical shaker typically operating at 20 Hz.

Figure 1(a) shows the time-resolved reflectivity changes at different pump power densities. The period of phonon oscillation is prolonged and its decay time is shortened with fluence. Vertical lines are located at the peak positions of the coherent phonon signal for the lowest fluence, and the change in peak positions with the oscillation period is distinctly observed. The corresponding Fourier transformed (FT) spectra are shown in Fig. 1(b). The peak frequency of the A_{1g} mode down-shifts and the spectrum shape is asymmetrically broadened to the lower frequency side.

The effect of anharmonicity of the lattice potential on softening of the A_{1g} mode is examined by controlling the phonon amplitude. The width of the pump pulse is adjusted by a prism pair, while the width of the probe pulse is maintained at 100fs. As the pump pulse width increases with the period of phonon oscillation, the amplitude of the coherent phonon drastically decreases. Figure 2(a) shows the coherent phonon signal for three pump pulse widths at a fluence of $7.0\text{ mJ}/\text{cm}^2$. The pump pulse width is evaluated by the width of the cross-correlation trace with probe-pulse and the time traces are labeled with these values. The corresponding cross-correlation traces are displayed in the inset. The amplitude of the phonon oscillation decreases by several times with the pump pulse width; however, the temporal profiles show negligible change. Figure 2(b) shows the corresponding Fourier power

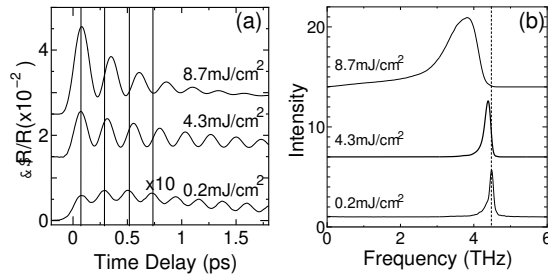


FIG. 1. (a) Time-resolved reflectivity changes at three pump fluences 0.2, 4.3, and $8.7\text{ mJ}/\text{cm}^2$. (b) Corresponding Fourier transformed power spectra.

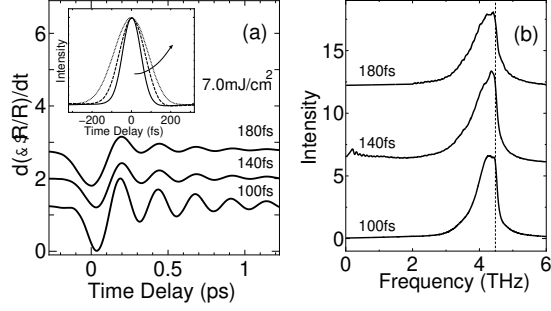


FIG. 2. Dependence of time derivative of reflectivity change on pump pulse width. (a) Temporal profiles for three pump pulse widths. Inset shows cross-correlation trace of pump and probe pulses. (b) Corresponding Fourier power spectra.

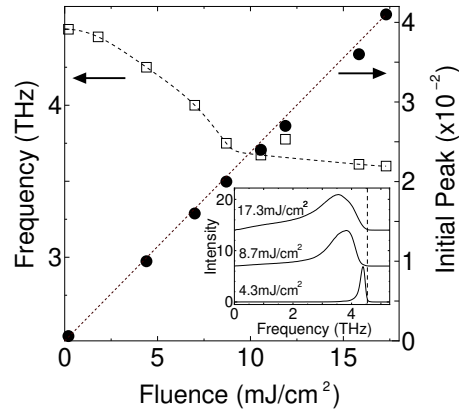


FIG. 3. Fluence dependence of initial frequency of oscillation (open squares) and height of initial peak (filled circles). Inset shows the Fourier power spectra at three pump fluences of 4.3, 8.7, and 17.3 mJ/cm^2 .

spectra obtained after removing the monotonic component. We also verified the dependence on the pump pulse width at higher fluences up to $17.3 \text{ mJ}/\text{cm}^2$, which is immediately below the damage threshold, and found that the temporal profile shows no significant change. It is clearly shown that the softening of coherent phonons is mostly determined by the accumulation of the pump pulse energy and not by the anharmonicity of the lattice potential.

To analyze the time-dependent frequency shift, we numerically fit the data over a monocyte of phonon oscillation with a function expressed as the sum of damping oscillation and a single exponential decay, and determine the instantaneous frequency. The region of the monocyte is selected approximately by the naked eye, and the frequency thus obtained is insensitive to the detail of the selection.

Open squares shown in Fig. 3 indicate the fluence dependence of initial frequency of the coherent phonon obtained by monocycle fitting. The frequency superlinearity decreases with fluence and shows saturation above 10 mJ/cm^2 . Excitation exceeding 20 mJ/cm^2 leads to optical damage of the sample. Filled circles in Fig. 3 indicate the fluence dependence of the height of the initial peak. The figure shows that the initial peak height increases linearly with fluence, which indicates that there is no significant absorption saturation. Therefore, the saturation of frequency shift originates from a purely internal mechanism. Fourier power spectra at the corresponding fluence is displayed in the inset of Fig. 3. The spectrum shows a large frequency shift and broadening as the fluence increases from 4.3 to 8.7 mJ/cm^2 . Compared with the spectrum at 8.7 mJ/cm^2 , the frequency shift of the spectrum at 17.3 mJ/cm^2 is saturated, although remarkable growth of the low frequency component materializes.

Figure 4 shows time evolutions of the amplitude and frequency of the coherent A_{1g} phonon for two fluences. Although the amplitude decreases almost exponentially with a decay constant of 0.4 ps^{-1} at 0.2 mJ/cm^2 , it shows an accelerated decay for the first 6 ps at 8.7 mJ/cm^2 , as shown in Fig. 4(a). The time dependence of frequency at 8.7 mJ/cm^2 indicates an abrupt change and a slight overshoot of the phonon frequency around the time delay of 2 ps in contrast to the flat time evolution at 0.2 mJ/cm^2 , as shown in Fig 4(b). At higher fluences, an abrupt change in frequency also appears around the time delay

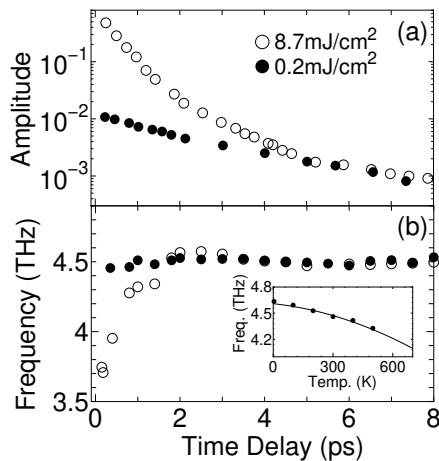


FIG. 4. Time evolutions of amplitude (a) and frequency (b) of coherent A_{1g} phonon for two fluences. The inset represents the temperature dependence of A_{1g} phonon frequency. Filled circles and open circles correspond to pump fluences of 0.2 and 8.7 mJ/cm^2 , respectively.

of 2 ps and becomes more discontinuous. After these transient responses, the frequency reaches a thermal equilibrium value of 4.50 THz, which lasts onward and the corresponding temperature is very close to room temperature. These experimental results, the saturation behavior of the softening and the unusual time evolution of phonon frequency, indicate that the mechanism of the softening process involves structural change rather than carrier-phonon interaction.

The change in the phonon frequency of the semi-metal that is initiated by the structural change under a high-pressure condition was extensively studied by Raman scattering and pump-probe experiments [17–19]. Figure 5 shows the comparison of the fluence dependence of the initial frequency of the coherent phonon with the uniaxial pressure dependence of the static phonon frequency measured by Raman scattering [18]. Crosses in the figure indicate the pressure dependence of the Raman peak frequency, and the pressure is indicated in the upper horizontal axis. Vertical dashed lines located at the pressures of 7.2 and 9.0 GPa correspond to the phase boundaries of Sb-I (hexagonal setting), Sb-IV, and Sb-II (host-guest structure). Filled circles indicate the pump fluence dependence of the phonon frequency, and the fluence is indicated in the lower horizontal axis. We set the conversion ratio of fluence to pressure as 0.9 GPa per 1.0 mJ/cm² so that the two curves overlap. Surprisingly, not only the decreases in super linearity at the Sb-I phase but also the saturation behavior at phase IV show extremely good agreement with the fluence dependence. This correspondence between the transient frequency and static pressure shifts of the phonon frequency clearly

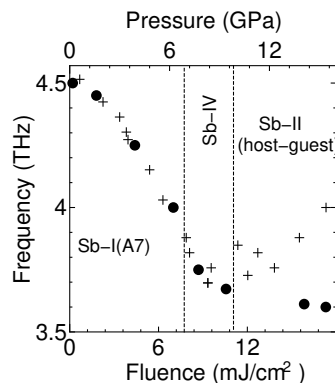


FIG. 5. Comparison of fluence and pressure dependences of phonon frequency. Crosses show pressure dependence of Raman frequencies for Sb. Filled circles show pump fluence dependence of coherent phonon frequencies for Sb.

indicates that the optical high density excitation generates a compressed state whose pressure is proportional to the fluence. Since there is no absorption saturation, as shown in Fig. 3, the disagreement of the frequency of the coherent phonon corresponding to the Sb-II phase could be explained by the formation of a quasi-stable state instead of a host-guest structure.

In contrast to the generally accepted idea that high density excitation weakens the covalent bond and the lattice undergoes the same expansion process as it undergoes when subject to a heating condition, time-resolved electron diffraction measurements have revealed instantaneous contraction of the atomic distance in graphite [2, 20]. Theoretically, the contraction in graphite [21] and the mechanism is now considered as the efficient LA phonon emission by the double resonant Raman process [22, 23]. A similar mechanism is also expected in our case; the lattice contraction explains the good correspondence between the fluence and pressure dependences of the phonon frequency, as shown in Fig. 5.

From the result of the optically generated high-pressure state, the following consideration is provided for the energy balance and the surface dynamics. The conventional material parameters used below are taken from the literature [24]. The sheet energy density of the strain is roughly expressed as $u = p^2 d / 2C_{33}$, where p is the pressure, d is the penetration depth, and C_{33} is the elastic modulus along the c -axis. Here, we calculate the strain energy density at the excitation density of 10 mJ/cm^2 . Using the pressure p of 9.0 GPa , the elastic modulus C_{33} of 44.6 GPa , and the optical penetration depth of 13 nm , the resultant strain energy density is 1.2 mJ/cm^2 . p is deduced from the frequency shift shown in Fig. 5; the elastic modulus C_{33} is obtained from the ultrasonic measurement; and the optical penetration depth is defined as the inverse of the absorption coefficient ($1/\alpha$) of the amorphous film of antimony at a wavelength of 790 nm . Since the photoabsorbed energy is determined as 3.0 mJ/cm^2 from the optical reflectivity of 70% , it is concluded that a large amount of the absorbed energy is converted into strain energy for the lattice, which is consistent with the X-ray experimental result [25]. It is well known that a strain pulse with a picosecond duration can be generated by irradiating a metal film or a semiconductor with intense femtosecond laser pulses and that it propagates into the sample [26–28]. Because our experimental conditions are very close to this situation, a strain pulse is also expected, and the lattice contraction corresponds to the initial stage of the strain pulse. The spatial size of the strain pulse estimated by the optical penetration depth d is 13 nm , and the acoustic velocity v of antimony along the c -axis is about 2584 m/s . Therefore, the escape time of the

strain pulse from the optical penetration layer is calculated as 5.0 ps. The complete recovery from phonon softening and the small temperature increase observed after 5 ps, as shown in Fig. 4, are satisfactorily explained by the strain pulse, which carries away the structural deformation and the associated energy from the surface. Further theoretical and experimental research is needed to clarify the dynamics of highly photoexcited solid surfaces. It is strongly emphasized that the high-pressure Raman scattering experiment is very powerful for understanding high density excitation phenomena.

In conclusion, we have investigated the impulsive softening process in antimony by using a precise measurement system based on rapid scan and microscope optics. The detailed analysis of the instantaneous frequency shift yields unexpected findings. The fluence dependence of the initial frequency is strongly correlated with the high-pressure Raman scattering experiment and the time evolution of the phonon frequency shows an abrupt change and overshoot. These results clearly indicate that the highly excited surface layer undergoes contraction and successive expansion processes that leads to ablation. Transient high pressure associated with lattice contraction represents the extreme reduction in the phonon frequency and the time evolution of the phonon frequency indicates the lattice deformation dynamics. Simple estimation of the energy balance reveals that most of the photo-injected energy is converted to lattice strain energy and the duration of the softening process is consistent with the exit time of the strain pulse propagating deep into the sample.

The authors thank Professor Takashi Kozasa and Dr. T. Yanagisawa for stimulating discussions.

* mis@phys.sci.hokudai.ac.jp

- [1] A. Pashkin, C. Kübler, H. Ehrke, R. Lopez, A. Halabica, R. F. Haglund, R. Huber, and A. Leitenstorfer, *Phys. Rev. B* **83**, 195120 (2011).
- [2] F. Carbone, P. Baum, P. Rudolf, and A. H. Zewail, *Phys. Rev. Lett.* **100**, 035501 (2008).
- [3] C. E. Otis and R. W. Dreyfus, *Phys. Rev. Lett.* **67**, 2102 (1991).
- [4] W. Hu, Y. C. Shin, and G. King, *Phys. Rev. B* **82**, 094111 (2010).
- [5] K. Sokolowski-Tinten, J. Bialkowski, M. Boing, A. Cavalleri, and D. von der Linde, *Phys. Rev. B* **58**, R11805 (1998).

- [6] W.-L. Chan, R. S. Averback, D. G. Cahill, and A. Lagoutchev, *Phys. Rev. B* **78**, 214107 (2008).
- [7] D. A. Kleinman and R. C. Miller, *Phys. Rev. B* **32**, 2266 (1985).
- [8] A. K. Nowak, E. Gallardo, H. P. van der Meulen, J. M. Calleja, J. M. Ripalda, L. González, and Y. González, *Phys. Rev. B* **83**, 245447 (2011).
- [9] G. C. Cho, W. Kütt, and H. Kurz, *Phys. Rev. Lett.* **65**, 764 (1990).
- [10] T. Pfeifer, W. Kütt, H. Kurz, and R. Scholz, *Phys. Rev. Lett.* **69**, 3248 (1992).
- [11] T. Mishina, K. Nitta, and Y. Masumoto, *Phys. Rev. B* **62**, 2908 (2000).
- [12] T. K. Cheng et al., *Ultrafast Phenomena IX*, P. F. Barbara and W. H. Knox, Springer Series in Chemical Physics, Vol. 60 (Springer, Berlin, 1994), p. 301.
- [13] S. Hunsche, K. Wienecke, T. Dekorsy, and H. Kurz, *Phys. Rev. Lett.* **75**, 1815 (1995).
- [14] M. Hase, M. Kitajima, S. Nakashima, and K. Mizoguchi, *Phys. Rev. Lett.* **88**, 067401 (2002).
- [15] E. D. Murray, S. Fahy, D. Prendergast, T. Ogitsu, D. M. Fritz, and D. A. Reis, *Phys. Rev. B* **75**, 184301 (2007).
- [16] D. M. Fritz, D. A. Reis, B. Adams, R. A. Akre, J. Arthur, C. Blome, P. H. Bucksbaum, A. L. Cavalieri, S. Engemann, S. Fahy, R. W. Falcone, P. H. Fuoss, K. J. Gaffney, M. J. George, J. Hajdu, M. P. Hertlein, P. B. Hillyard, M. H. Hoegen, M. Kammler, J. Kaspar, R. Kienberger, P. Krejcik, S. H. Lee, A. M. Lindenberg, B. McFarland, D. Meyer, T. Montagne, É. D. Murray, A. J. Nelson, M. Nicoul, R. Pahl, J. Rudati, D. P. S. H. Schlarb, K. Sokolowski-Tinten, T. Tschentscher, D. von der Linde, and J. B. Hastings, *Science* **315**, 633 (2007).
- [17] X. Wang, K. Kunc, I. Loa, U. Schwarz, and K. Syassen, *Phys. Rev. B* **74**, 134305 (2006).
- [18] O. Degtyareva, V. V. Struzhkin, and R. J. Hemley, *Solid State Commun.* **141**, 164 (2007).
- [19] M. Kasami, T. Ogino, T. Mishina, S. Yamamoto, and J. Nakahara, *J. Lumin.* **119-120**, 428 (2006).
- [20] R. K. Raman, Y. Muraoka, C.-Y. Ruan, T. Yang, S. Berber, and D. Tománek, *Phys. Rev. Lett.* **101**, 077401 (2008).
- [21] H. O. Jeschke, M. E. Garcia, and K. H. Bennemann, *Phys. Rev. Lett.* **87**, 015003 (2001).
- [22] F. Carbone, G. Aubeck, A. Cannizzo, F. V. Mourik, R. Nair, A. Geim, K. Novoselov, and M. Chergui, *Chem. Phys. Lett.* **504**, 37 (2011).
- [23] R. Saito, A. Jorio, A. G. Souza Filho, G. Dresselhaus, M. Dresselhaus, and M. A. Pimenta, *Phys. Rev. Lett.* **88**, 027401 (2002).

- [24] Optical transitions with 800 nm light would occur dominantly at the L point (interband transition). H. Lehmann, in Landolt-Bornstein, New Series, edited by O. Madelung (Springer, Berlin, 1983), Vol. 17.
- [25] D. A. Reis, M. F. DeCamp, P. H. Bucksbaum, R. Clarke, E. Dufresne, M. Hertlein, R. Merlin, R. Falcone, H. Kapteyn, M. M. Murnane, J. L. T. Missalla, and J. S. Wark, Phys. Rev. Lett. **86**, 3072 (2001).
- [26] J. J. Baumberg, D. A. Williams, and K. Köhler, Phys. Rev. Lett. **78**, 3358 (1997).
- [27] M. Kasami, T. Mishina, S. Yamamoto, and J. Nakahara, J. Lumin. **108**, 291 (2004).
- [28] A. V. Akimov, A. V. Scherbakov, D. R. Yakovlev, C. T. Foxon, and M. Bayer, Phys. Rev. Lett. **97**, 037401 (2006).